DOI 10.5012/bkcs.2011.32.6.1851

Articles

Zeolite-catalyzed Isomerization of 1-Hexene to *trans*-2-Hexene: An ONIOM Study

Yan-Feng Li, Ji-Qin Zhu, Hui Liu,* Peng He, Peng Wang,† and Hui-Ping Tian†

*State Key Laboratory of Chemical Resource Engineering, Beijing University of Chemical Technology, Beijing 100029, P. R. China. *E-mail: hliu@mail.buct.edu.cn*
† Research Institute of Petroleum Processing, SINOPEC, Beijing 100083, P. R. China
Received December 6, 2010, Accepted March 3, 2011

Details of the double-bond isomerization of 1-hexene over H-ZSM-5 were clarified using density functional theory. It is found that the reaction proceeds by a mechanism which involves the Brønsted acid part of the zeolite solely. According to this mechanism, 1-hexene is first physically adsorbed on the acidic site, and then, the acidic proton transfers to one carbon atom of the double bond, while the other carbon atom of the double bond bonds with the Brønsted host oxygen, yielding a stable alkoxy intermediate. Thereafter, the Brønsted host oxygen abstracts a hydrogen atom from the C_6H_{13} fragment and the C–O bond is broken, restoring the acidic site and yielding *trans*-2-hexene. The calculated activation barrier is 12.65 kcal/mol, which is in good agreement with the experimental value. These results well explain the energetic aspects during the course of double-bond isomerization and extend the understanding of the nature of the zeolite active sites.

Key Words : Hexene, ZSM-5, Double-bond isomerization, Active site, Density functional theory

Introduction

Within the context of catalysis by solid catalytic materials, the hydrocarbon conversion processes such as oligomerization, cyclization, polymerization, disproportionation, cracking and double-bond isomerization, are of great importance in the petrochemical industry.[1] For these processes zeolites are commonly used catalytic materials.[2,3] Among a variety of zeolites, ZSM-5 zeolite shows moderate Brønsted acidity, good mechanical and thermal stability, and unique shape-selective properties.[4-7] The Brønsted acidity is originated from the bridging hydroxyl groups formed by substitution of trivalent aluminum atoms for tetravalent silicon atoms in its framework, in which place, various acid-catalyzed reactions may take place under different reaction conditions by means of the bifunctional (acid-base) nature of the zeolite active sites, namely, the combinative roles of both the Brønsted acid sites and the neighboring framework oxygen atoms which play the role of basic sites. The acid moiety acts as a proton donor, while the basic moiety either stabilizes intermediate protonated species or favors the proton abstraction from the transition state.[8] Understanding the mechanism of the reaction occurring on the acid sites of the zeolite is essential not only for the research of the catalysis of zeolites, but also for the development and design of new, more effective, and possibly selective catalytic materials.

In view of the practical importance of double-bond isomerization of linear olefins, namely to produce the desired products with improved octane numbers,[9-11] this paper is mainly concerned with the double-bond isomerization of hexene on ZSM-5 zeolite. In the reaction, the double bond at the terminal position of 1-hexene migrates, giving rise to *trans*-2-hexene *via* an isomerization mechanism. So the reaction system constitutes also as a model system for us to probe the nature of the Brønsted acid sites and the reaction mechanism. Although extensive experimental studies have been performed to identify the reaction mechanism,[12-25] they often disagree on the intermediates and elementary steps involved in the reaction. Lechert *et al*.[12] and Bezouhanova *et al*.[13] reported upon a basis of IR spectroscopy investigation that the double-bond isomerization of 1-hexene involves formation of carbenium ion intermediate on H-ZSM-5. Campbell[19] and Pines[20] reached the conclusion that the isomerization of 1-hexene to 2-hexene proceeds *via* deprotonation from the adsorbed carbenium ion. On the contrary, Burwell *et al*.[21] demonstrated that the olefin isomerization might happen *via* a different mechanism with no carbenium ion formed. In the first sight, this is in accordance with the fact that to date no free carbenium ions are experimentally observed on the surface of acidic zeolites.[26-28] Moreover, Brouwer[22] found that double-bond shift occurs and follows a concerted reaction mechanism; and in situ spectroscopic studies (solid-state NMR and IR) of the interaction of Brønsted acid sites with hexene indicated that protonation of adsorbed olefins results in the formation of covalent alkoxide species.[29-31]

In order to explain the experimental results on the reaction mechanism, theoretical methodologies were used also.[8,32-34] Benco *et al*.[32] carried out molecular dynamics simulations and found in the IR spectra no distinctive feature evidencing

the existence of the protonated species. They thus suggested that future simulations should focus on the alkoxy species. In their theoretical studies on the mechanism of zeolite-catalyzed reactions of linear olefins, Bhan *et al*.[33] confirmed the formation of the alkoxide intermediates and the π-complex. Moreover, Kazansky[8] proposed that the double-bond isomerization of the olefin involves the formation of a surface alkoxy group by proton addition from the zeolite to the double bond of the olefin and the following decomposition of this alkoxy intermediate. In our previous work,[34] in an attempt to ascertain the reaction pathway for the double-bond isomerization of 1-hexene to *trans*-2-hexene on H-ZSM-5 zeolite, we also pointed out that the reaction proceeds by a bifunctional (acid-base) mechanism of active centers with the formation of covalent alkoxy intermediates.

In summary, the discrepancies existing among the different experimental and theoretical investigations on the intermediates and elementary steps involved in the reaction highlights the need for a detailed and true explanation of the elementary steps for the double-bond isomerization of 1-hexene to *trans*-2-hexene on the surface of H-ZSM-5 zeolite.

The major objective of the present paper is to ascertain the reaction pathway for the H-ZSM-5 zeolite-catalyzed double-bond isomerization of 1-hexene to *trans*-2-hexene *via* formation of alkoxy species on the framework oxygen that originally hosts the Brønsted acid proton. We attain this goal by applying density functional theory (DFT) that yields the geometries, vibrational frequencies, and characterization of reactants, products, reaction intermediates, and transition states, and the activation energies for the process. By the method we adopted, we hope to make detailed comparison and re-evaluation of the existing experimental observations and computational results and therefore to render it evident of the reaction pathway.

Models and Computational Methods

It is generally recognized that the cluster approach is particularly suited to obtain information pertinent to the local electronic and structural properties of the zeolite as well as the potential energy surface characterizing interactions with guest molecules.[33,35] Hybrid methods, especially, the Our-own-*N*-layered Integrated molecular Orbital + molecular Mechanics (ONIOM) methods,[36,37] were found to be appropriate in describing the acidic site of the zeolite surface and yielding reasonable estimates of the system energetics, yet they are capable of reasonable simplification for the computation of the complex zeolite-guest molecule system in which numerical and computation capacities are highly demanding. On account of the above consideration, in this work we constructed a 54T cluster model to represent the local structures of H-ZSM-5 zeolite, with the effects of the zeolite framework being implicitly included in subsequent calculations (see Fig. 1). In the 54T cluster, the Al is situated at the T11 site in the straight channels. For computational efficiency, the 54T cluster model is subdivided into two layers according to the two-layer ONIOM scheme. The

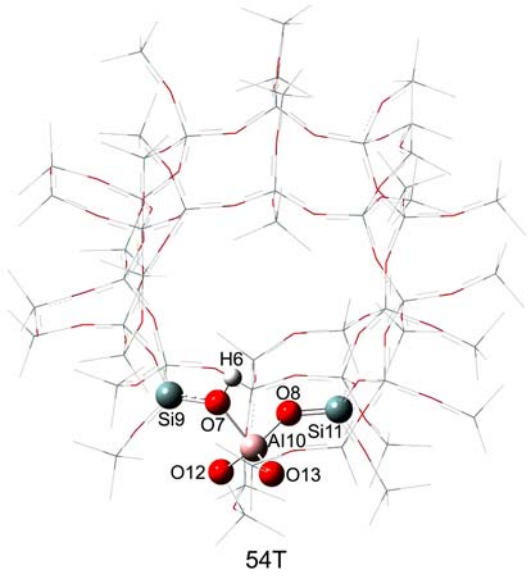

Figure 1. Calculated structure for 54T cluster.

inner layer consists of 3T atoms and accounts for the bifunctional nature of the zeolite active sites by incorporating both the Brønsted acidic hydroxyl group and one neighboring basic oxygen, and is considered as the active region. The outer layer, up to 54T, represents the confinement effect of the zeolite pore structure, which include the 10-membered ring channel containing the active region. Hydrogen atoms are used as link atoms and to saturate the dangling bonds of the outer layer.

To validate the feasibility of the model for ZSM-5 zeolite, we calculated the vibrational frequencies of the 54T model. In the case of the isolated 54T cluster, the calculated stretching frequency of the acidic H–O bond is 3623 cm^{-1}, while the experimental values were around 3610-3623 cm^{-1}.[13,38-40] Besides, the optimized geometric data of the 54T cluster were found to be in general agreement with the previous computational results concerning H-ZSM-5[36,37] and those of the crystal structure of H-ZSM-5 found in XRD study.[41] Therefore, it is a good justification to use the 54T model to represent a real ZSM-5 zeolite.

All calculations in this work were performed by the Gaussian 03 program.[42] The inner layer and hexene were treated quantum chemically at the B3LYP[43,44] level of DFT using the 6-31G(d, p) basis set for all types of atoms, while the outer layer was treated with the universal force field (UFF).[45] The DFT-based method was chosen because, among the methodologies for which calculations on clusters are feasible, it is the one that gives the best results when compared to the ab initio methods.[46,47] The B3LYP functional was chosen because, among the presently available functionals, it has been demonstrated to give the best description for DFT treatment of reaction profiles in zeolite systems.[48] It has been reported that the UFF force field is the practical choice for the low-level methodology when the high-level region is treated by the DFT/B3LYP method.[49] During the structure optimization, only the active region is allowed to relax since it has been pointed out that full relaxation of

zeolite clusters can lead to structures that deviate largely from the experimental zeolite geometries.[50] At this computational level, vibrational frequencies were calculated to identify the nature of the stationary points and obtain the zero-point-energy (ZPE) corrections. The vibrational frequencies were scaled by a factor of 0.9614[51] for a better comparison with the observed values. The minimum energy paths were obtained by the intrinsic reaction coordinate (IRC) calculations with a gradient step size of 0.05 $(amu)^{1/2}$ bohr.

Results and Discussion

Physisorption of 1-Hexene and *trans*-2-Hexene. In this section, we show the interaction of 1-hexene and *trans*-2-hexene with the Brønsted acidic site to form physisorbed π-complexes. After optimizing the geometries of the reactant and product separately, we obtained the equilibrium geometries of the complexes. Figure 2 shows the resultant structures for the adsorbed 1-hexene (H1) and *trans*-2-hexene (H2) on the zeolite surface. The optimized values of the main parameters are listed in Table 1 respectively for 1-hexene, *trans*-2-hexene, the 54T cluster and the complexes.

From Figure 2 and Table 1, it is seen that the main characteristics of the cluster geometry after formation of the complexes are those related to the orientation of the hydrogen atom in the bridging hydroxyl group toward the double bond of hexene. The acidic proton points at the nontotally equidistant position of the C=C bond, being closer to C1 than to C2 in H1 and closer to C2 than to C3 in H2. At the same time, the structural deformation of the 54T cluster in the complexes is rather modest compared with its isolated structure. For instance, the Si9–O7 and O7–Al10 bond lengths decrease only by 0.05 and 0.04 Å from the 54T cluster to H1, respectively, and these differences are negligibly small. The angle of θ(Si9–O7–Al10) is 126.6º and 127.1º from the 54T to H1, and increases very little. Moreover, in the complexes practically no change in the geometry of 1-hexene and *trans*-2-hexene occurs. For instance, the C1–C2 bond length is 1.3330 Å in the isolated 1-hexene and increases by about 0.01 Å in H1, while their C3–H5 bond lengths are almost equal. The bond angle of θ(C1–C2–C3) increases only by 0.4º from the isolated 1-hexene to H1. The only observable difference is that the C=C and O–H bond lengths in the complexes are about 0.01 Å longer than those in the isolated systems, respectively, suggesting that the adsorption slightly weakens the C=C bonds and acidic O–H bonds. The structural analyses indicate that hexene is adsorbed to the zeolite acid site weakly.

The net charges of the functional atoms of the two complexes hardly vary when compared to those of the isolated systems, and consequently, only a small increase of about +0.07e, respectively, in the total charge of 1-hexene and *trans*-2-hexene is induced by the surface adsorption. Addi-

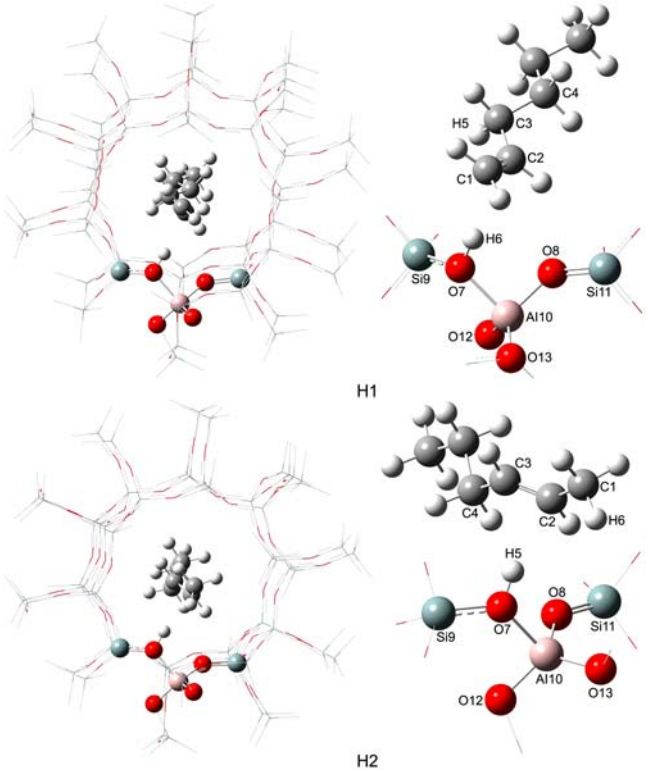

Figure 2. Calculated structures for adsorbed 1-hexene (H1) and *trans*-2-hexene (H2).

Table 1. Main parameters (distances in Å, angles in º, frequencies in cm^{-1}, charges in *e*) of 1-hexene, *trans*-2-hexene, 54T cluster and complexes

	1-hexene	*trans*-2-hexene	54T	H1	H2
C1–C2	1.3330	1.5017		1.3401	1.5041
C2–C3	1.5037	1.3354		1.5055	1.3421
C3–C4	1.5402	1.5040		1.5417	1.5056
C1–H6		1.0976		2.3103	1.0967
C2–H5	2.1362				2.1716
C2–H6		2.1584		2.4155	
C3–H5	1.1006			1.0968	2.4435
C1–C2–C3	125.4	125.3		125.8	124.8
C2–C3–C4	113.1	125.4		112.7	126.8
C1–H6–O7				167.9	
C3–H5–O7					158.0
H5–O7					0.9873
H6–O7			0.9790	0.9866	
Si9–O7			1.6960	1.6914	1.6887
O7–Al10			1.8669	1.8628	1.8693
Al10–O8			1.7258	1.7158	1.7141
O8–Si11			1.6119	1.6021	1.6009
O7–Al10–O8			86.6	90.6	90.9
Si9–O7–Al10			126.6	127.1	128.6
$\nu_{O7\text{-}H5}$					3305
$\nu_{O7\text{-}H6}$			3623	3341	
$\nu_{C=C}$	1662	1688		1637	1659
q_{C1}	–0.245	–0.350		–0.300	–0.352
q_{C2}	–0.021	–0.063		–0.051	–0.125
q_{H5}					0.371
q_{H6}			0.386	0.372	

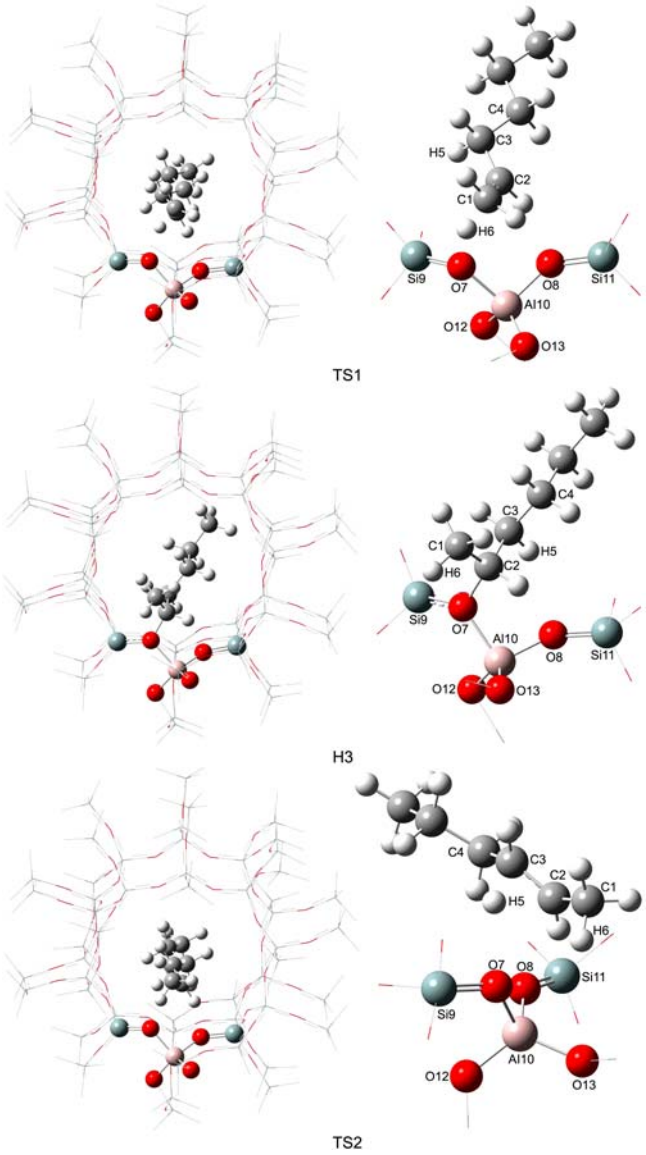

Figure 3. Calculated structures for alkoxy intermediate (H3) and transition states (TS1 and TS2).

tionally, computations of the stretching frequencies of the C=C bonds show that the C=C stretching frequencies of the isolated 1-hexene and *trans*-2-hexene are 1662 and 1688 cm^{-1}, while the values for the H1 and H2 are 1637 and 1659 cm^{-1}, respectively. Computations of the stretching frequencies of the O–H bonds show that the O–H stretching frequencies of the H1 and H2 are 3341 and 3305 cm^{-1}, respectively. The C=C stretching frequency of the H1 is in good accordance with the available experimental value (1620-1650 cm^{-1})[12] and the calculated O–H stretching frequency of the H1 also is in reasonable agreement with the observed value, around 3310 cm^{-1}.[52] The charge analyses and the calculated small frequency downshift of the C=C and O–H bonds further indicate that hexene is in far contact with the acidic proton and adsorbed to the zeolite acid site weakly.

The above results indicate that the 1-hexene and *trans*-2-hexene molecules are physically adsorbed on the zeolite acid sites with the formation of π-complexes. This is in accordance with the existing experimental observations[12,13,22] and theoretical calculations.[8,32-34]

Table 2. Main parameters (distances in Å, angles in °, frequencies in cm^{-1}, charges in *e*) of alkoxy intermediate and transition states

	TS1	H3	TS2
C1–C2	1.4200	1.5258	1.4762
C2–C3	1.4621	1.5262	1.4017
C3–C4	1.5592	1.5403	1.5234
C1–H6	1.1564	1.0902	
C2–H5			1.5322
C2–H6	1.8544		
C3–H5	1.1034	1.0941	1.1964
C2–O7	2.7689	1.5426	2.6859
C1–C2–C3	126.5	116.4	124.2
C2–C3–C4	110.8	112.0	124.4
C1–H6–O7	144.4		
C3–H5–O7			149.6
H5–O7			2.1228
H6–O7	1.8295		
Si9–O7	1.6229	1.7188	1.6190
O7–Al10	1.7693	1.8653	1.7635
Al10–O8	1.7539	1.7158	1.7530
O8–Si11	1.5955	1.6056	1.5935
O7–Al10–O8	94.1	99.8	94.8
Si9–O7–Al10	125.9	125.5	125.3
$\nu_{C1\text{-}C2}$	1498		
$\nu_{C2\text{-}C3}$			1518
q_{H6}	0.279		
q_{H5}			0.252

Double-bond Isomerization. Protonation of the substrate molecule is the initial step of hydrocarbon conversion on acidic zeolite catalysts.[53] Starting from the geometry of the H1, we searched for the transition state TS1, through which H1 is protonated by the acidic proton of the zeolite and forms a covalent alkoxy intermediate H3. Figure 3 presents the optimized structures of the transition states and alkoxy intermediate. The optimized values of the main parameters of the transition states and alkoxy intermediate are listed in Table 2. In what follows, we discuss the different aspects of double-bond isomerization based on these geometric and electronic results.

In the transition state TS1 there is an obvious tendency of protonation of 1-hexene, and the proton H6 of the OH acidic group begins to transfer to the C1 atom, while the C2 atom begins to bond with the original host oxygen O7 of the acidic proton H6. A key observation from the elementary step is that only the Brønsted acidic hydroxyl group functions to activate the 1-hexene. This scenario is different from the bifunctional nature of the zeolite active sites which combines the roles of both the Brønsted acidic hydroxyl group and the neighboring basic oxygen.[34] The structural parameters of the C_6H_{13} fragment in TS1 are very close to the classical form of the 2-hexyl secondary carbenium ion,[54] suggesting that the TS1 exhibits significant ionic characteri-

stics. In this structure, the H6–O7 bond is actually broken (1.8295 Å), whereas the bond between C1 atom and the proton H6 is not yet completely formed (1.1564 Å). A significant lengthening of the C1–C2 bond is observed varying from the double bond value of 1.3401 Å to 1.4200 Å (a distance intermediate between single bond and double bond). At the same time, the neighboring C2–C3 single-bond distance decreases to 1.4621 Å. The calculated stretching frequency of the C1–C2 in the TS1 is 1498 cm^{-1}, which is close to the values, 1515 cm^{-1} and 1510 cm^{-1}, reported by Lechert *et al*.[12] and Bezouhanova *et al*.,[13] respectively.

Charge distribution calculations according to the Mulliken population analyses give a further insight into the high carbocation character of the TS1. The total positive charge on the C_6H_{13} fragment is +0.795e, and mainly localized on the C2 and H6 atoms. The net atomic charge on H6 (+0.279e) is between those of the hydrogen atoms bonded to carbon atoms (about +0.149e) and that of the proton of the cluster hydroxyl group (+0.372e). The negative charge on the cluster is symmetrically distributed between the two oxygen atoms, O7 and O8, and this charge delocalization is clearly reflected in the optimized geometry. According to the above analyses it can be inferred that the TS1 for the elementary step exhibits carbenium ion characteristics; in other words, the TS1 is carbenium-ion-like, which is in agreement with the results reported in the literature.[12,13,19,34]

We then analyze the formation reaction of the alkoxy intermediate H3 by means of the geometry of the TS1. Because the loss of the acidic proton in the zeolite catalytic sites generates a negative charge on the zeolite framework and charge separation is energetically costly in acidic zeolite, the protonated 1-hexene in the transition state structure is not stable in the form of a carbenium ion. At the same time, the formation of an alkoxy bond between a carbon atom of the protonated 1-hexene and an oxygen atom of the zeolite catalytic site can stabilize the positive charge. Hence, the protonated 1-hexene is quickly transformed to a stabilized alkoxy intermediate H3 by forming a covalent bond to the Brønsted host oxygen O7. Namely, the alkoxide species is formed on the framework oxygen O7 that originally hosts the Brønsted acid proton H6. The change of the C2–O7 distance in the H1 and TS1 confirms that the primary reaction coordinate involves the C2–O7 bond formation.

The structural characteristics of the alkoxy intermediate H3 is explanatory *via* an analysis of the resulting geometry and its net atomic charges. The calculated C2–O7 bond length in the H3 is 1.5426 Å, being close to the mean length of these bonds in esters or alcohols,[8,55] and the geometry of the C2 atom resembles that of a tetrahedrally coordinated carbon.[33] This indicates that the H3 assumes the typical structural parameters of covalent organic compounds. The optimized C–C bond lengths in the H3, all of which are between 1.5258 and 1.5403 Å, are typical values of covalent organic compounds. At the same time, the relatively low positive net charge of the C_6H_{13} fragment (+0.465e), the charge of C2 atom bonded to O7 atom (+0.183e), and the C1 and C3 atom charges (–0.344e and –0.210e, respectively) are similar to those of esters and alcohols which are covalent.[8,55] All these geometric and electronic data confirm that the H3 is structurally covalent.

The formation of the H3 is accompanied by significant structural changes of the 54T cluster. The most important changes observed in the geometry of the 54T cluster are the angles around the O7 atom bonded to the 2-hexyl group, with theoretical variation up to 5° in order to accomodate the more voluminous C_6H_{13} fragment. In addition, the Si9–O7 and O7–Al10 bond lengths increase by 0.0959 and 0.0960 Å, and the Al10–O8 bond length decreases by 0.0381 Å, respectively. Comparison with the structural parameters of the TS1 shows that a strong interaction exists between the C2 and O7 atoms and the intermediate is highly stable alkoxide species.

We next searched for the transition state TS2, through which H3 is decomposed resulting in the adsorbed *trans*-2-hexene on the zeolite surface. The optimized structure of the TS2 is plotted in Figure 3, and the optimized values of the main parameters of the TS2 are tabulated in Table 2. It is seen that the TS2 exhibits geometric and electronic properties resembling those of the TS1. Typically, the decomposition of the H3 associates with the stretching of the C2–O7 bond and the tendency to deprotonate. The C2–O7 bond distance is significantly lengthened from 1.5426 to 2.6859 Å and the C2–C3 bond distance decreases to 1.4017 Å. The C3–H5 and H5–O7 bond lengths are 1.1964 and 2.1228 Å, respectively. According to the Mulliken population analyses, the total positive charge (+0.825e) on the C_6H_{13} fragment is mainly located on the C2 and H5 atoms, and the negative charge on the zeolite fragment is distributed between the O7 and O8 atoms.

Lastly, the framework oxygen O7 that originally hosts the Brønsted acid proton H6 abstracts a hydrogen atom, H5, from the C3 atom through the TS2, which restores the acid site of the zeolite. Meanwhile, the C2–O7 bond is ruptured and the C2–C3 bond length decreases to the length of C=C double bond, which leads to the formation of the adsorbed *trans*-2-hexene. This completes the course of the double-bond isomerization of 1-hexene to *trans*-2-hexene on the surface of H-ZSM-5 zeolite.

Vibrational Analyses of Transition-state Structures and Intrinsic Reaction Coordinate Paths. To investigate the vibrational modes of the transition-state structures, we performed the frequency calculations for the TS1 and TS2. For TS1 there is only one imaginary vibrational mode (319 cm^{-1}) associated with the movement of the acidic proton H6 between the oxygen atom O7 of the cluster and the carbon atom C1 of 1-hexene, while the C2 atom interacts with the Brønsted host oxygen O7 of the cluster. At this point we can conclude that the reactant and the product of TS1 are H1 and H3, respectively, and the TS1 is just one of the transition states of the reaction. Analogous to the TS1, the TS2 has an imaginary vibrational frequency (403 cm^{-1}) only, and the animation of the only one imaginary vibrational mode manifests the change in the C2–O7, C3–H5 and H5–O7 bond distances, which confirms that the TS2 is just another

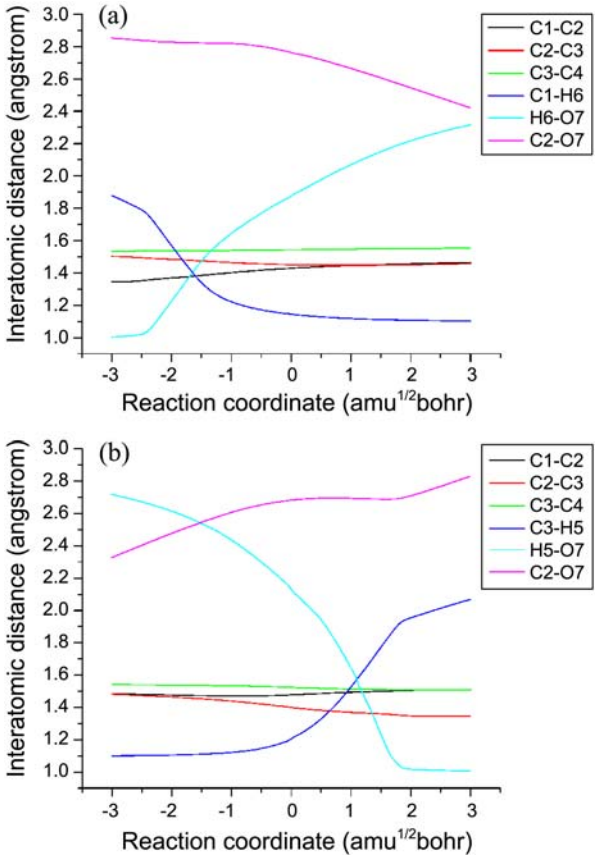

Figure 4. Changes of the interatomic distances as functions of the reaction coordinate for the double-bond isomerization of 1-hexene to *trans*-2-hexene. A—TS1; and B—TS2.

transition state of this reaction.

In order to confirm the reaction pathways from the transition states to the products and reactants, IRC calculations of the TS1 and TS2 were carried out with a gradient step size of 0.05 (amu)$^{1/2}$ bohr at the same computational level. The changes of the main interatomic distances along the IRC of the TS1 and TS2 are plotted in Figure 4(a) and Fig. 4(b), respectively. Inspecting Figure 4(a) shows that, as the reaction proceeds towards the product, the acidic proton H6 bound to the oxygen atom O7 attacks the 1-hexene molecule and bonds to the carbon atom C1, and simultaneously, the carbon atom C2 moves towards the original host oxygen O7 of the acidic proton H6 resulting in the C2–O7 covalent bond, and the C1–C2 bond length increases to the length of C–C single bond. In short, the acidic proton H6 transfer is accompanied with the formation of the alkoxy intermediate. On the other hand, Figure 4(b) indicates that the hydrogen atom H5 bound to the carbon atom C3 moves away from the C_6H_{13} fragment towards the framework oxygen O7 that originally hosts the Brønsted acid proton H6. At the same time, the C2–O7 bond is elongated until the bond is broken, and the C2–C3 bond length shortens to the length of C=C double bond. In particular, the hydrogen atom H5 transfer reconstructs the acid site of the zeolite, while the C_6H_{13} fragment, after loosing the hydrogen atom H5, gives rise to the *trans*-2-hexene molecule. The IRC analyses further

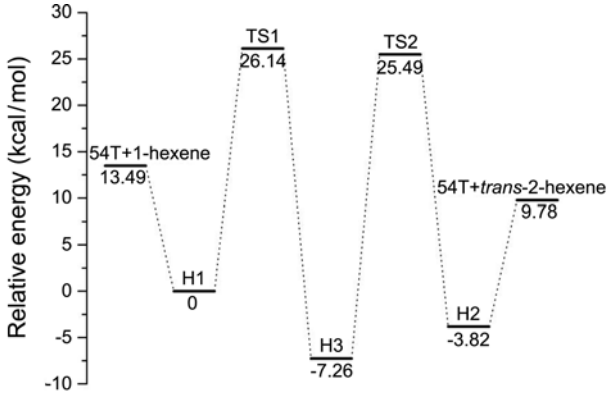

Figure 5. Calculated energy profile for the double-bond isomerization of 1-hexene to *trans*-2-hexene including ZPE values. The energy of H1 is taken as the origin of energies.

confirm that the TS1 and TS2 belong to the transition states of the isomerization pathway of 1-hexene to *trans*-2-hexene.

Potential Energy Profile. Figure 5 shows the potential energy profile for the double-bond isomerization of 1-hexene to *trans*-2-hexene over the H-ZSM-5 zeolite including ZPE values. It is observed that the calculated adsorption energies of 1-hexene and *trans*-2-hexene are 13.49 and 13.60 kcal/mol, respectively. They are close to the experimental adsorption energies (11.23-13.15 kcal/mol) reported by Pariente *et al*.[56] From the relative energies of stationary points depicted in Figure 5 it can be seen that the rate-determining step of the proposed mechanism is the conversion of the H3 into the H2 through the TS2, and therefore, the real activation barrier for this reaction should be viewed as the energy difference between H3 and TS2 (32.75 kcal/mol). This is due to the high stability of the H3, whose strong covalent C2–O7 bond has to be broken for the reaction to take place, and this requires the high activation energy. This value is comparable to that we reported previously upon the bifunctional mechanism (30.92 kcal/mol).[34] In addition, the calculated apparent activation energy is 12.65 kcal/mol, which is the energy difference between the TS1 and separated reactants (isolated 1-hexene and the 54T cluster). This value is in good agreement with the average experimental activation energy value of 13.38 kcal/mol reported by Clark and Subramaniam[57] and close to the calculated activation energy values (10.80 kcal/mol reported by Bhan *et al*.[33] and 10.47 kcal/mol reported by us,[34] respectively) for the bifunctional mechanism. The conformity of the activation energy values indicates that the proposed reaction pathway is reasonable and is competitive with the bifunctional pathway.

Conclusions

In this paper, a systematic DFT study on the double-bond isomerization reaction of 1-hexene to *trans*-2-hexene in H-ZSM-5 zeolite, modeled by a 54T cluster, were performed. The geometries of reactants, products, intermediates, and transition states have been optimized. The stationary points have been characterized by frequency calculations, and IRC

calculations have also been performed. Reaction energy diagram of the reaction and estimates of the activation energy barriers are obtained.

Our DFT calculations demonstrate that the 1-hexene and *trans*-2-hexene molecules are physically adsorbed on the zeolite acid sites with the formation of the π-complexes. The adsorption energies of 1-hexene and *trans*-2-hexene are 13.49 and 13.60 kcal/mol, respectively. For adsorption of 1-hexene, the computed stretching frequencies of the C=C bond and the acidic OH group are in conformity with the available experimental data.

An important result obtained in this study is that the double-bond isomerization of 1-hexene to *trans*-2-hexene proceeds with the formation of alkoxy species on the framework oxygen that originally hosts the Brønsted acid proton. According to this mechanism, the acidic proton of the zeolite transfers to one carbon atom of the double bond of adsorbed 1-hexene, while the other carbon atom of the double bond of adsorbed 1-hexene bonds with the Brønsted host oxygen, yielding a stable alkoxy intermediate. Thereafter, the C–O bond of the alkoxy intermediate is broken and the Brønsted host oxygen abstracts a hydrogen atom from the C_6H_{13} fragment, restoring the zeolite active site and yielding adsorbed *trans*-2-hexene. In contrast to the commonly accepted bifunctional nature of the zeolite active sites, only the Brønsted acid part works in this mechanism.

The DFT-calculated activation energies for the whole process are also given. The real activation energy for this pathway (32.75 kcal/mol) compares well with that for the bifunctional pathway (30.92 kcal/mol). In addition, the apparent activation energy for this isomerization reaction (12.65 kcal/mol) has been compared with the available experimental value (13.38 kcal/mol), which shows a good agreement. Thus, we conclude the mechanism that does not involve the bifunctional nature of the zeolite active sites but rather the Brønsted acid sites solely is feasible. The results are useful to get further insight into the nature of the zeolite active sites.

Supporting Information. Tables of the coordinates for all the calculated systems. The supporting materials are available *via* the Internet *http://newjournal. kcsnet.or.kr*.

Acknowledgments. The financial supported by the National Basic Research Program of China (973 Project No. 2010CB732301) and the National Scientific Funding of China (No. 20706005) are gratefully acknowledged.

References

1. Milas, I.; Nascimento, M. A. C. *Chem. Phys. Lett.* **2001**, *338*, 67.
2. Venuto, P. B. *Microporous Mater.* **1994**, *2*, 297.
3. Ding, B. J.; Huang, S. P.; Wang, W. C. *Appl. Surf. Sci.* **2008**, *254*, 4944.
4. Corma, A. *Chem. Rev.* **1995**, *95*, 559.
5. Stöcker, M. *Micropor. Mesopor. Mater.* **1999**, *29*, 3.
6. Zardkoohi, M.; Haw, J. F.; Lunsford, J. H. *J. Am. Chem. Soc.* **1987**, *109*, 5278.
7. Jin, H.; Prasetyanto, E. A.; Jiang, N.; Oh, S.-M.; Park, S.-E. *Appl. Surf. Sci.* **2010**, *256*, 5508.
8. Kazansky, V. B. *Acc. Chem. Res.* **1991**, *24*, 379.
9. Gates, B. C. *Catalytic Chemistry*; John Wiley and Sons: New York, 1991.
10. Dunning, H. N. *Ind. Eng. Chem.* **1953**, *45*, 551.
11. Bounaceur, R.; Warth, V.; Sirjean, B.; Glaude, P. A.; Fournet, R.; Battin-Leclerc, F. *Proc. Combust. Inst.* **2009**, *32*, 387.
12. Lechert, H.; Dimitrov, C.; Bezuhanova, C.; Nenova, V. *J. Catal.* **1983**, *80*, 457.
13. Bezouhanova, C.; Lechert, H.; Taralanska, G.; Meyer, A. *React. Kinet. Catal. Lett.* **1989**, *40*, 209.
14. Neurock, M.; van Santen, R. A. *Catal. Today* **1999**, *50*, 445.
15. Keane, M. A.; Alyea, E. C. *J. Mol. Catal. A: Chem.* **1996**, *106*, 277.
16. Abbot, J.; Wojciechowski, B. W. *J. Catal.* **1984**, *90*, 270.
17. Abbot, J.; Corma, A.; Wojciechowski, B. W. *J. Catal.* **1985**, *92*, 398.
18. Anderson, J. R.; Chang, Y. F.; Western, R. J. *J. Catal.* **1989**, *118*, 467.
19. Campbell, I. M. *Catalysis at Surfaces*; Springer: 1988.
20. Pines, H. *The Chemistry of Catalytic Hydrocarbon Conversions*; Academic Press: New York, 1981.
21. Burwell, R. L.; Shim, K. C.; Rowlinsox, H. C. *J. Am. Chem. Soc.* **1957**, *79*, 5142.
22. Brouwer, D. M. *J. Catal.* **1962**, *1*, 22.
23. Rogers, D. W.; Crooks, E.; Dejroongruang, K. *J. Chem. Thermodyn.* **1987**, *19*, 1209.
24. Perez-Luna, M.; Cosultchi, A.; Toledo-Antonio, J. A.; Diaz-Garcia, L. *Catal. Lett.* **2009**, *128*, 290.
25. Naragon, E. A. *Ind. Eng. Chem.* **1950**, *42*, 2490.
26. Ishikawa, H.; Yoda, E.; Kondo, J. N.; Wakabayashi, F.; Domen, K. *J. Phys. Chem. B* **1999**, *103*, 5681.
27. Geobaldo, F.; Spoto, G.; Bordiga, S.; Lamberti, C.; Zecchina, A. *J. Chem. Soc., Faraday Trans.* **1997**, *93*, 1243.
28. Kondo, J. N.; Wakabayashi, F.; Domen, K. *J. Phys. Chem. B* **1998**, *102*, 2259.
29. Haw, J. F.; Richardson, B. R.; Oshiro, I. S.; Lazo, N. D.; Speed, J. A. *J. Am. Chem. Soc.* **1989**, *111*, 2052.
30. Aronson, M. T.; Gorte, R. J.; Farneth, W. E.; White, D. *J. Am. Chem. Soc.* **1989**, *111*, 840.
31. Kondo, J. N.; Wakabayashi, F.; Domen, K. *Catal. Lett.* **1998**, *53*, 215.
32. Benco, L.; Demuth, T.; Hafner, J.; Hutschka, F.; Toulhoat, H. *J. Catal.* **2002**, *205*, 147.
33. Bhan, A.; Joshi, Y. V.; Delgass, W. N.; Thomson, K. T. *J. Phys. Chem. B* **2003**, *107*, 10476.
34. Li, Y. F.; He, P.; Zhu, J. Q.; Liu, H.; Shao, Q.; Tian, H. P. *J. Mol. Struc: THEOCHEM.* **2010**, *940*, 135.
35. Rozanska, X.; van Santen, R. A.; Hutschka, F.; Hafner, J. *J. Am. Chem. Soc.* **2001**, *123*, 7655.
36. Lomratsiri, J.; Probst, M.; Limtrakul, J. *J. Mol. Graphics Modell.* **2006**, *25*, 219.
37. Namuangruk, S.; Khongpracha, P.; Pantu, P.; Limtrakul, J. *J. Phys. Chem. B* **2006**, *110*, 25950.
38. Jacobs, P. A.; Martens, J. A.; Weitkamp, J.; Beyer, H. K. *Faraday Discuss. Chem. Soc.* **1981**, *72*, 353.
39. Mortier, W. J.; Sauer, J.; Lercher, J. A.; Noller, H. *J. Phys. Chem.* **1984**, *88*, 905.
40. Trombetta, M.; Armaroli, T.; Alejandre, A. G.; Solis, J. R.; Busca, G. *Appl. Catal. A: Gen.* **2000**, *192*, 125.
41. Lermer, H.; Draeger, M.; Steffen, J.; Unger, K. K. *Zeolites* **1985**, *5*, 131.
42. Frisch, M. J.; Trucks, G. W.; Schlegel, H. B. *et al. Gaussian 03, Revision D.01*; Gaussian Inc., Wallingford CT, 2004.
43. Lee, C.; Yang, W.; Parr, R. G. *Phys. Rev. B* **1988**, *37*, 785.
44. Becke, A. D. *Phys. Rev. A* **1988**, *38*, 3098.
45. Rappe, A. K.; Casewit, C. J.; Colwell, K. S.; Goddard, W. A.; Skiff, W. M. *J. Am. Chem. Soc.* **1992**, *114*, 10024.

46. de Albuquerque Lins, J. O. M.; Nascimento, M. A. C. *J. Mol. Struc: THEOCHEM.* **1996**, *371*, 237.
47. Esteves, P. M.; Nascimento, M. A. C.; Mota, C. J. A. *J. Phys. Chem. B* **1999**, *103*, 10417.
48. Zygmunt, S. A.; Mueller, R. M.; Curtiss, L. A.; Iton, L. E. *J. Mol. Struc: THEOCHEM.* **1998**, *430*, 9.
49. Panjan, W.; Limtrakul, J. *J. Mol. Struct.* **2003**, *654*, 35.
50. Brand, H. V.; Curtiss, L. A.; Iton, L. E. *J. Phys. Chem.* **1993**, *97*, 12773.
51. Scott, A. P.; Radom, L. *J. Phys. Chem.* **1996**, *100*, 16502.
52. Föttinger, K.; Kinger, G.; Vinek, H. *Appl. Catal. A: Gen.* **2003**, *249*, 205.
53. Krossner, M.; Sauer, J. *J. Phys. Chem.* **1996**, *100*, 6199.
54. In order to facilitate the analysis of the transition states, we have calculated the geometry and the electronic structure of the 2-hexyl secondary carbenium ion at the 6-31G(d, p) level.
55. Hehre, W. J.; Radom, L.; Schleyer, P. v. R.; Pople, J. A. *Ab Initio Molecular Orbital Theory*; Wiley: New York, 1986.
56. Pariente, S.; Trens, P.; Fajula, F.; Di Renzo, F.; Tanchoux, N. *Appl. Catal. A: Gen.* **2006**, *307*, 51.
57. Clark, M. C.; Subramaniam, B. *AIChE J.* **1999**, *45*, 1559.

DOI 10.5012/bkcs.2011.32.6.

Supporting Information

Zeolite-catalyzed Isomerization of 1-hexene to *trans*-2-hexene: An ONIOM Study

Yan-Feng Li, Ji-Qin Zhu, Hui Liu,* Peng He, Peng Wang,† and Hui-Ping Tian†

*State Key Laboratory of Chemical Resource Engineering, Beijing University of Chemical Technology, Beijing 100029, P. R. China. *E-mail: hliu@mail.buct.edu.cn*

† Research Institute of Petroleum Processing, SINOPEC, Beijing 100083, P. R. China

Received December 6, 2010, Accepted March 3, 2011

Table S1. The coordinates for the inner layer of 54T cluster

Atomic Number	Coordinates (Angstroms)		
	X	Y	Z
H6	-2.30009674	0.01643561	-2.72492922
O7	-2.48609800	0.12659800	-3.67972800
O8	-1.93624900	-2.25909500	-3.27592200
Si9	-1.71941376	1.45310142	-4.40709402
Al10	-2.90406500	-1.52082700	-4.49925800
Si11	-1.96006100	-3.67218900	-2.50084000
O12	-2.13704300	-1.07314300	-5.94450000
O13	-4.49183400	-2.08772600	-4.54804100

Table S2. The coordinates for the inner layer of adsorbed 1-hexene (H1)

Atomic Number	Coordinates (Angstroms)		
	X	Y	Z
C1	-2.061714	0.003124	-0.409201
C2	-0.822049	-0.309059	-0.811382
C3	0.415832	0.527531	-0.626449
C4	1.649253	-0.311253	-0.236511
H5	0.633277	1.026662	-1.578582
H6	-2.299466	-0.061860	-2.706265
O7	-2.535130	0.065299	-3.655809
O8	-1.803249	-2.348574	-3.312337
Si9	-1.811926	1.438460	-4.328379
Al10	-2.800997	-1.583895	-4.480070
Si11	-1.781889	-3.752302	-2.540355
O12	-2.083541	-1.047220	-5.930412
O13	-4.350784	-2.257684	-4.553027

Table S3. The coordinates for the inner layer of adsorbed *trans*-2-hexene (H2)

Atomic Number	Coordinates (Angstroms)		
	X	Y	Z
C1	-4.215025	0.037474	-0.047495
C2	-2.815410	-0.223464	-0.532418
C3	-1.787552	0.629241	-0.399501
C4	-0.356160	0.384074	-0.796701
H5	-2.532798	0.088395	-2.662839
H6	-4.953218	-0.091262	-0.848234
O7	-2.568037	0.126372	-3.648818
O8	-1.879327	-2.304582	-3.254883
Si9	-1.783940	1.469361	-4.307080
Al10	-2.871692	-1.545312	-4.428221
Si11	-1.880249	-3.710440	-2.489106
O12	-2.157590	-1.088543	-5.903084
O13	-4.452450	-2.152732	-4.459611

Table S4. The coordinates for the inner layer of transition state (TS1)

Atomic Number	Coordinates (Angstroms)		
	X	Y	Z
C1	0.111427	-7.636120	-0.831858
C2	0.305044	-6.267946	-1.158907
C3	-0.542930	-5.148116	-0.753117
C4	0.323471	-3.925534	-0.322007
H5	-1.086436	-4.848862	-1.665524
H6	-0.238347	-7.875024	-1.907845
O7	-0.095352	-7.379336	-3.663138
O8	2.346227	-6.549161	-3.338675
Si9	-1.426269	-6.692615	-4.288314
Al10	1.465696	-7.550178	-4.478266
Si11	3.756161	-6.545579	-2.591955
O12	1.002837	-6.821459	-5.959833
O13	2.277768	-9.050836	-4.550328

Table S5. The coordinates for the inner layer of alkoxy intermediate (H3)

Atomic Number	Coordinates (Angstroms)		
	X	Y	Z
C1	-0.629078	-8.689641	-1.501733
C2	0.146275	-7.525553	-2.111503
C3	-0.015987	-6.170576	-1.428158
C4	0.425595	-6.211533	0.046903
H5	0.593359	-5.446384	-1.977150
H6	-0.879307	-9.438322	-2.253680
O7	-0.091550	-7.395386	-3.630152
O8	2.451889	-6.584924	-3.403197
Si9	-1.520739	-6.709595	-4.294605
Al10	1.548667	-7.538978	-4.506775
Si11	3.831856	-6.540239	-2.583599
O12	0.988238	-6.838109	-5.956123
O13	2.201393	-9.094107	-4.612975

Table S6. The coordinates for the inner layer of transition state (TS2)

Atomic Number	Coordinates (Angstroms)		
	X	Y	Z
C1	-0.108294	-9.024258	-0.882906
C2	0.452260	-7.669218	-1.052907
C3	-0.169159	-6.497703	-0.598778
C4	0.507984	-5.134676	-0.532923
H5	-0.509230	-6.687077	-1.730099
H6	-0.318438	-9.442679	-1.871591
O7	-0.072530	-7.417074	-3.675009
O8	2.354461	-6.592338	-3.300004
Si9	-1.389596	-6.731451	-4.320414
Al10	1.492554	-7.568583	-4.473533
Si11	3.766371	-6.552216	-2.562292
O12	1.054280	-6.853335	-5.967921
O13	2.318861	-9.068223	-4.526878